https://doi.org/10.5194/egusphere-2024-1873
Preprint. Discussion started: 1 July 2024

Seasonality and scenario dependence of rapid Arctic sea ice loss events in CMIP6 simulations

Annelies Sticker[1,*], François Massonnet[1], Thierry Fichefet[1], Patricia DeRepentigny[1], Alexandra Jahn[2,3], David Docquier[4], Christopher Wyburn-Powell[2,3], Daphne Quint[2], Erica Shivers[2], and Makayla Ortiz[2]

[1]Earth and Life Institute, Earth and Climate, UCLouvain, Louvain-la-Neuve, Belgium
[2]Department of Atmospheric and Oceanic Sciences, University of Colorado Boulder, Boulder, CO, USA
[3]Institute for Arctic and Alpine Research, University of Colorado Boulder, Boulder, CO, USA
[4]Royal Meteorological Institute of Belgium, Brussels, Belgium
[*]Corresponding author: Annelies Sticker (annelies.sticker@uclouvain.be)

Abstract.

The end-of-summer Arctic Ocean is projected to face at least one occurrence of practically ice-free conditions (sea ice extent <1 million km^2) by the middle of the century under all Climate Model Intercomparison Project phase 6 (CMIP6) scenarios. Climate models indicate that this transition toward a nearly ice-free Arctic Ocean in late summer will be punctuated by rapid ice loss events (RILEs), i.e., reductions in sea ice extent that occur at a much faster rate than expected from the forced contribution. The extreme sea ice loss associated with RILEs in climate models is larger than what has been observed since the start of the satellite era (-0.28 million km^2 per year over 2001–2008). As such, it could lead to a much faster transition toward practically ice-free conditions than expected based on a linear trend. RILEs are not well understood and it is currently impossible to predict their occurrence a season to several years ahead. It is therefore essential to improve our understanding of these events. This study presents the first comprehensive analysis of RILEs in a diverse set of 26 CMIP6 models, including 5 large ensembles, following both low and high warming scenarios over the period from 1970 to 2100. Our analysis shows that RILEs are expected to occur year-round. However, the timing and duration of the events are found to be season-dependent, with less frequent but longer-lived RILEs in winter and spring, and more frequent but shorter-lived RILEs in summer and autumn under a high emission scenario. In addition, we find that the warming scenario has a greater influence on RILE characteristics in the winter/spring season than in the summer/autumn season. Our results also emphasize that model uncertainty is larger regarding the probability and characteristics of RILEs for winter/spring events compared to summer/autumn ones. Finally, while the initial sea ice extent at which RILEs are triggered depends on whether they occur in September or March, the initial sea ice volume is similar for both months, which emphasizes the critical role of sea ice thickness as a preconditioning factor for RILEs. Based on CMIP6 models, there is 63% chance that at least one summer RILE starts before 2030 in September. The study of RILEs is particularly opportune as, after more than ten years of relatively stable conditions between 2012–2023, the current summer Arctic sea ice state has an increased probability to be on the verge of a rapid reduction for the coming decade.

https://doi.org/10.5194/egusphere-2024-1873
Preprint. Discussion started: 1 July 2024

1 Introduction

The state of the sea ice cover in the Arctic stands as an important sign of the region's transition to a warmer climate, highlighting its role both as an indicator and driver of global change (Serreze et al., 2009; Serreze and Barry, 2011; Taylor et al., 2013; Meredith et al., 2019). Over the past few decades, the Arctic has undergone large changes, leaving the sea ice in a new state (Landrum and Holland, 2020). The sea ice extent (SIE) at the end of summer has diminished by 12.5% per decade between 1979 and 2023 relative to the 1981–2010 average (Fetterer et al., 2017). The decrease in Arctic SIE does not only occur in September but also throughout the year (Onarheim et al., 2018), and in addition to reduction in extent, the sea ice cover is also much younger and thinner, making the ice that survives year-round more vulnerable to atmospheric and oceanic variability (Stroeve and Notz, 2018).

The long-term negative trend in Arctic SIE is largely attributed to the increase in greenhouse gas concentrations in the atmosphere (Stroeve and Notz, 2015; Meredith et al., 2019). However, superimposed upon this trend is a interannual to decadal variability leading to periods of relative stability interrupted by abrupt sea ice declines (Kay et al., 2011; Swart et al., 2015; Baxter et al., 2019). As an example, Arctic sea ice retreated more than three times faster in the first decade of the 21st century (2001–2010: -1.7 million km^2/decade) than it did in the last two decades of the 20th century (1981–2000: -0.5 million km^2/decade). More recently, the September sea ice extent trend over 2011–2020 has been relatively weak (-0.2 million km^2/decade). Altogether, the mechanisms underlying these fluctuations remain largely unclear. Polyakov et al. (2023) stated a connection between the Arctic Dipole and fluctuations in Arctic SIE on sub-decadal to decadal timescales, suggesting a 15-year cycle that could explain the recent slowdown in sea ice decline. They attributed this deceleration to enhanced redistribution of freshwater into the Amerasian Basin caused by anomalous winds and increased stratification that strongly weakened oceanic heat fluxes. These findings suggest that large declines in sea ice may occur when the Arctic Dipole undergoes a reversal in its cycle. On the other hand, Baxter et al. (2019) showed that interdecadal variations in summer sea ice are partly caused by teleconnections that arise from changes in sea surface temperature in the east-central tropical Pacific Ocean. These teleconnections are made possible by a Rossby wave train that travels to the Arctic and leads an internal mode that connects the pole to lower latitudes. According to the authors, the Arctic sea ice loss and warming that occurred between 2007 and 2012 were exacerbated by this mode (Baxter et al., 2019). Additionally, Francis and Wu (2020) underscored the influence of atmospheric states conducive to low pressure formation over the Arctic, leading to increased cloud cover, reduced insolation, and winds favoring ice expansion. These atmospheric states weakened in the early 2020s, potentially setting the stage for a new record minimum sea ice extent.

Accelerated sea ice retreat during one or several consecutive seasons can have profound impacts on the Arctic environment. During such periods, accessibility of shipping routes can be greatly enhanced for several months of the year and winter sea ice might become thin enough to let light icebreakers cruise to the Arctic safely all year round (Crawford et al., 2021). Ecosystems can also feel the effects of sudden multi-year sea ice retreats, as the length of the sea ice season exerts a first-order control on the amount of light reaching phytoplankton, the building blocks of the Arctic food web (Arrigo and van Dijken, 2011; Wassmann et al., 2011). Finally, by exposing more of the Arctic Ocean to the atmosphere for several years in a row, extended periods of large sea ice decline can enhance the ice-albedo feedback and lead to increased temperature and evaporation, which could

https://doi.org/10.5194/egusphere-2024-1873
Preprint. Discussion started: 1 July 2024

translate to extreme weather events in the terrestrial regions of the Arctic periphery (e.g., Alaska, Svalbard, coastal Siberia; Screen et al., 2015; Delhaye et al., 2023; Lawrence et al., 2008).

The concept of a rapid ice loss event (RILE) was first proposed by Holland et al. (2006) when they identified periods of abrupt reduction in summer Arctic sea ice in seven simulations of the Community Climate System Model (CCSM) version 3. Several modeling studies on RILEs have since followed (e.g., Lawrence et al., 2008; Holland et al., 2008; Döscher and Koenigk, 2013; Paquin et al., 2013; Auclair and Tremblay, 2018; Mioduszewski et al., 2019; Rieke et al., 2023) and they all project that RILEs will become more prevalent in the upcoming decades as sea ice variability rises. Despite the previous studies about RILEs, we still currently lack a year-round overview of the properties of RILEs and the mechanisms underlying the occurrence of RILEs remain poorly understood, posing challenges in accurately predicting their onset from one season to several years in advance.

The latest generation of models participating in the Coupled Model Intercomparison Project (CMIP6) exhibit several improvements in their representation of global and polar climate. These models show a more realistic estimate of the sensitivity of September Arctic sea ice area to CO_2 emissions and improved representation of sea ice dynamics (SIMIP Community, 2020; Watts et al., 2021), making it worthwhile to reassess Arctic sea ice variability through the lens of RILEs. In this study, we present the first investigation of RILEs year-round using a multi-model ensemble gathering 26 different climate models as well as 5 large ensembles (Sect. 2). The role of different emission scenarios is also assessed by using two future CMIP6 scenarios, a low-emitting greenhouse gas emission scenario (SSP1-2.6) and a high-emitting scenario (SSP5-8.5). We first assess the seasonality of RILEs, highlighting large differences in the characteristics of RILEs that occur in the first versus last six months of the year (Sect. 3.1). We also look at the probability of RILEs in CMIP6 simulations (Sect. 3.2). Then we focus on the timing of RILEs as well as the SIE and total sea ice volume (SIV) at which RILEs start, focusing on September and March RILEs (Sect. 3.3). Finally, we discuss the implications of our results and conclude in Sect. 4 and 5.

2 Data and Methods

2.1 Data

We analyze data from the first ensemble member of 26 CMIP6 models (see Table 1) that were chosen based on the availability of sea ice variables such as SIE, sea ice concentration (SIC) and SIV. The nominal horizontal resolution of the ocean/sea ice component from the different CMIP6 models varies between 25 and 250 km, with the majority using a resolution of 100 km (Table 1). We use output from historical simulations, which cover the period 1850 to 2014, except for the EC-Earth3 large ensemble spanning from 1970 to 2014. We also employed two sets of climate projections following low and high warming scenarios, specifically SSP1-2.6 and SSP5-8.5, which correspond to a top-of-atmosphere radiative forcing in 2100 of 2.6 and 8.5 $\mathrm{W/m^2}$ with respect to pre-industrial levels, respectively (O'Neill et al., 2016). The climate projections cover the period 2015 to 2100, except for the CAMS-CSM1-0 model (model #4 in Table 1) which ranges from 2015 to 2099. We only use the years covered by all models and, as such, our study focuses on the time period 1970–2099.

https://doi.org/10.5194/egusphere-2024-1873
Preprint. Discussion started: 1 July 2024

In addition to the CMIP6 multi-model ensemble that allows for a detailed investigation of model uncertainty, we also analyze historical and SSP5-8.5 simulations from 5 large ensembles to better understand the role of internal climate variability on our results: ACCESS-ESM1-5 (40 ensemble members; Ziehn et al., 2020), CanESM5 (25 ensemble members; Swart et al., 2019), EC-Earth3 (50 ensemble members; Wyser et al., 2021), MIROC6 (50 ensemble members; Shiogama et al., 2023), and MPI-ESM1-2-LR (30 ensemble members; Olonscheck et al., 2023). These large ensembles and their ensemble size were chosen based on the availability of sea ice variables. Using multiple large ensembles offers a robust comparison of forced responses and internal climate variability across models (Deser et al., 2020).

The primary sea ice output used in this study is the Arctic SIE, labeled as *siextentn* in the CMIP6 output. In cases where *siextentn* was unavailable, we computed the SIE time series using the SIC data, labeled as *siconc* in the CMIP6 output. SIE is calculated as the total area of all grid cells where SIC exceeds 15%. SIE is a commonly used metric for model comparisons (Shu et al., 2020; Watts et al., 2021; Shen et al., 2021) and our choice of SIE metrics aligns with the existing definitions of RILEs to maintain consistency (Auclair and Tremblay, 2018). However, it is important to note that a limitation of SIE compared to sea ice area (SIA), as highlighted by Notz (2014), is its strong dependency on grid resolution. Nonetheless, we find that our conclusions using SIE are generally consistent with results using SIA. We also analyze SIV, labeled as *sivoln* in the CMIP6 output. If SIV was not available, we computed total Arctic SIV from sea ice thickness (SIT), labeled as *sivol* (grid cell-averaged ice thickness) or *sithick* (sea ice thickness averaged over the ice-covered portion of a grid cell) in the CMIP6 output. If only *sithick* was available, we converted it to volume by multiplying by SIC. By taking into account the vertical dimension, the SIV metric offers a more comprehensive representation of the condition of the Arctic sea ice cover as it relates more directly to the thermodynamic processes governing its evolution (Stroeve and Notz, 2015).

2.2 Model Evaluation

Climate models are powerful tools to analyze the mean state, trends, and variability of the climate system, and how those will evolve into the future. However, the reliability of the conclusions related to sea ice drawn from modeling studies is dependent on the accuracy of the representation of Arctic sea ice and the underlying physical processes embedded within models. To ensure the robustness of our results, we evaluate the performance of the sea ice simulations used in this study using the newly developed SITool (Lin et al., 2021). This tool is designed to assess the skill of CMIP6 simulations by comparing various sea ice metrics with observational references. To do so, we rely on observations of SIE and SIC obtained from the NASA Team (NSIDC-0051) dataset (Cavalieri et al., 1996) and reanalysis of SIT from PIOMAS (Schweiger et al., 2011). Observed SIC and SIT reanalysis data are available since 1979 and, as such, the evaluation of CMIP6 models focuses on the period 1979 to 2014.

SITool reveals noticeable differences between models of the multi-model ensemble in their representation of SIE (Fig.S1); however, the multi-model mean demonstrates a good performance relative to observational data for both March and September (Fig. 1a). Additionally, we find that the majority of CMIP6 models effectively replicate the mean and variability of SIC, SIE, and SIT, as well as the spatial distribution of the ice edge (Figs.S1 and S2). Note that some models exhibit larger disparities in one or more metrics when compared to observed references: BCC-CSM2-MR, CAMS-CSM1-0, NESM3, EC-Earth3, and

https://doi.org/10.5194/egusphere-2024-1873
Preprint. Discussion started: 1 July 2024

MIROC-E2SL. However, we find that screening out these models does not affect our conclusions (not shown) and, therefore, we have retained this subset of models for the analysis. We also conducted the same evaluation on all members of the five large ensembles for SIE and found that ACCESS-ESM1-5 and MPI-ESM1-2-LR demonstrate better performance in reproducing the mean state, standard deviation, and trend of Arctic sea ice extent, while CanESM5, EC-Earth3, and MIROC6 show slightly lower performance (Figs. 1b and S3). Specifically, CanESM5 exhibits a particularly negative trend during 1979 to 2014 compared to observations and MIROC6 shows a less negative trend compared to observations and greatly underestimates SIE from November to June (not shown).

2.3 Definition of RILEs

Several definitions exist in the scientific literature for RILEs in the Arctic, each emphasizing distinct criteria and temporal characteristics (Holland et al., 2008; Lawrence et al., 2008; Döscher and Koenigk, 2013; Paquin et al., 2013; Auclair and Tremblay, 2018; Mioduszewski et al., 2019; Rieke et al., 2023). Holland et al. (2006) used the rate of change exceeding a specific threshold, determined through the derivative of the 5-year mean smoothed time series of SIE. Based on this definition, a RILE is identified when sea ice loss surpasses 0.5 million km^2 per year, with the event's duration based on the period during which SIE decreases by more than 0.15 million km^2 per year. In contrast, Auclair and Tremblay (2018) defined rapid sea ice declines based on a period lasting at least 4 years, with the trend in the 5-year running mean minimum SIE consistently lower than -0.3 million km^2 per year. Döscher and Koenigk (2013) characterized a RILE as a drop in summer SIE exceeding 1.2 million km^2. As such, a RILE can manifest itself as a single large drop ("one-step event") or a series of up to three consecutive steps involving smaller year-to-year drops ("multi-year event"). Finally, Rieke et al. (2023) assessed rapid ice change events (RICEs) in the Barents Sea using 5-year linear trends of winter (November–April) SIA. RICEs are identified when trends exceed two standard deviations of the distribution of 5-year trends in the Community Earth System Model Large Ensemble (CESM-LE) between 2007 and 2025.

For this study, we use the definition from Auclair and Tremblay (2018), for which a RILE is a period lasting at least 4 years, during which the trend in the 5-year running mean minimum SIE is lower than -0.3 million km^2 per year. We chose this definition as it emphasizes the total amount of loss during a RILE, with the 5-year running mean filtering out interannual variability, as well as limits RILEs to events that last several years rather than single year events, thus focusing on events having a larger impact on climate, ecosystems, and society. We apply the definition from Auclair and Tremblay (2018) to all months of the year maintaining the same threshold. According to this definition, a RILE is even more extreme than the most rapid observed sea ice loss to date. Indeed, over the period 1979–2023, the observed SIE in the Arctic decreased by 0.039 million km^2 per year in March and by 0.079 million km^2 per year in September (Fetterer et al., 2017), with the most rapid sea ice decline in September reaching -0.28 million km^2 per year (for 2001–2008).

https://doi.org/10.5194/egusphere-2024-1873
Preprint. Discussion started: 1 July 2024

3 Results

3.1 Seasonality of RILEs

When examining the occurrence of RILEs throughout the year from 1970–2099, we find a distinct regime difference between the first and last six months of the year (Figs. 2 and 3). Indeed, the characteristics of RILEs (e.g., total number of RILEs simulated, duration over multiple years, and intra-seasonal consistency over several months during one year) are noticeably different between winter/spring and summer/fall RILEs, both under the high and low warming scenarios (Fig. 2). From January to June, very few RILEs are simulated by the CMIP6 multi-model ensemble between 1970 and 2050, with an increasing frequency toward the end of the 21st century under high warming scenario (SSP5-8.5) in about a third of the models (Fig. 2a,b). These winter and spring RILEs also exhibit intra-seasonal consistency, meaning that they extend over multiple months of the same year (see darker colors in Fig. 2a,b). For the low warming scenario (SSP1-2.6), only a few RILEs are simulated over the 130 years of our study period, indicating a large contribution from scenario uncertainty on the probability of occurrence of future winter and spring RILEs (Fig. 2e,f). In contrast, between July and December, RILEs are more abundant, though more short-lived, and appear to be randomly distributed throughout the time period when ice is present (1970 to consistently ice-free conditions; Jahn et al. (2024)) for both warming scenarios (Fig. 2c,d,g,h). We also see a smaller impact of the choice of future scenario on RILEs occurring in the last six months of the year, especially for summer RILEs (Jul-Aug-Sep; Fig. 2c,g). This is particularly striking for September RILEs (SRILEs hereafter), with no discernible influence of forcing on the total number of SRILEs simulated across the CMIP6 multi-model ensemble, their duration, as well as the number of SRILEs for one CMIP6 realization (Fig. 4e,f,g). This suggests that forcing factors predominantly influence winter and spring conditions, with little to no role on summer/autumn conditions.

This regime difference between winter and summer RILEs is also present in the large ensembles (Fig. 3). In addition, the large ensemble analysis reveals that internal climate variability uncertainty plays a minimal role for the seasonality, duration, and probability of occurrence of RILEs as these characteristics are found to be very similar between the five large ensembles and the CMIP6 multi-model ensemble (compare Figs. 4e,f,g and 5e,f,g). On the other hand, we see a large contribution of model uncertainty on the probability of occurrence of future winter RILEs (Fig. 3a,b,c,d,e), something that was already apparent in the CMIP6 multi-model ensemble under high warming scenario (Fig. 2a,b). Indeed, some models simulate a large number of winter RILEs across all ensemble members (CanESM5, ACCESS-ESM1-5, and EC-Earth3), whereas only a few winter RILEs are simulated for MPI-ESM1-2-LR and no RILE is simulated in March for MIROC6 (Fig. 5). This model uncertainty is also reflected in the timing when winter RILEs first occur as well as their intra-seasonal consistency for multiple months of the year (Fig. 3). In Sect. 3.3, we take a closer look at some important characteristics of RILEs that will shed light on the physical processes leading to this model uncertainty.

Because of the expected increase in sea ice variability as the thickness of the ice cover decreases (Holland et al., 2008) and the extreme sea ice loss associated with RILEs, one could expect an early transition toward consistently ice-free conditions in models that simulate many RILEs. However, we find no clear relationship between RILE occurrence and the timing of consistently September ice-free conditions, with instances of September ice-free conditions occurring at the end of multiple,

https://doi.org/10.5194/egusphere-2024-1873
Preprint. Discussion started: 1 July 2024

few, or no RILEs at all. Indeed, some models from the five large ensembles simulate many RILEs before reaching consistently September ice-free conditions (e.g., CanESM5, EC-Earth3, and ACCESS-ESM1-5), while others simulate only a few if any (e.g., MIROC6 and MPI-ESM1-2-LR; Fig. 3). We also find that some models start simulating winter RILEs immediately after the occurrence of consistently ice-free conditions in September (e.g., CanESM5), while for other models (e.g., ACCESS-ESM1-5, MIROC6, EC-Earth3), there is a lag of around 20–30 years between the timing of consistently ice-free conditions in September and the onset of winter RILEs. This confirms that uncertainty regarding the initiation of winter RILEs is large and is strongly model-dependent in addition to the choice of future scenario, as discussed above.

3.2 Probability of occurence of RILEs

The probability of having at least one SRILE (September RILE) over the period 1970–2099 in the CMIP6 multi-model ensemble is 92% for both scenarios, with a maximum of five SRILEs projected during this period for one single simulation (Fig. 4g). When looking at results from the large ensembles, we find disparities across models in terms of the probability of occurrence of SRILEs. There is a 78% probability of having at least one SRILE per simulation with the MIROC6 large ensemble, with 46% of simulations having only one RILE over the period 1970 to 2099. In contrast, the EC-Earth3 members show a 100% probability of having at least one SRILE over the same period, with 90% of simulations projected to have more than one SRILE (Fig. 5g). This range of results may be related to differences in SIE mean state, variability, and trends amongst models (Figs. 1 and S5). This again highlights the important role of model uncertainty and of the models' mean state, on the probability of occurrence of RILEs.

Interestingly, we find an increased probability of SRILE occurrence after a period of no sea ice loss (i.e., a 10-year period with a neutral or positive SIE trend; Fig. 6). Indeed, compared to the overall probability of seeing a RILE of 7%, the probability of a RILE occurrence following a stable period is around 20%, consistent across the CMIP6 multi-model ensemble (Fig. 6) and the five large ensembles (Fig.S6), and those differences are all highly significant (z score > 5). This result suggests that, after the recent positive trend of observed SIE over 2012–2023 (0.00168 million km^2 per year; Fetterer et al. (2017)), the probability of seeing a RILE in the near future is increased.

3.3 Mean State Influence on RILE Occurrence

SRILEs start occurring in the late 20$^{\text{th}}$ century and early 2000s for the CMIP6 multi-model ensemble (Fig. 4a). By 2025, 50% of SRILEs have already occurred and by 2070 all events have taken place for both scenarios. No SRILE occurs after consistently ice-free conditions occur in September (not shown). For the large ensembles, the initiation of SRILEs is similar to the CMIP6 multi-model ensemble: 50% of the total number of SRILEs have already occurred at the earliest by year 2020, as in CanESM5, and at the latest by 2040 for models such as MIROC6 and MPI-ESM1-2-LR (Fig. 5a). In these models, the timing of SRILEs is coherent with an increase in September SIE variability (Holland et al., 2008): sea ice variability in CanESM5 starts to increase around 2010 and peaks around 2025, whereas the peak in SIE variability for MIROC6 and MPI-ESM1-2-LR occurs about 20 years later (Fig. S5a).

https://doi.org/10.5194/egusphere-2024-1873
Preprint. Discussion started: 1 July 2024

Even though the timing of SRILEs varies by up to two decades across models, the peak of probability of RILEs' onset as a function of SIE is quite consistent for both the CMIP6 multi-model ensemble and large ensembles at slightly less than 4 million km^2 (Figs. 4b and 5b), which suggests that the dependence of RILEs' onset to the mean state is similar across models. This is also the SIE at which the large ensembles simulates the largest values of September sea ice variability (Fig. S5b). Interestingly, CanESM5 and EC-Earth3 show a two-peak distribution of September SIE at which RILEs begin and end (Fig. 5b,d). This could be explained by a split between early (1970–2020) and late (2020–2100) RILEs in these two models (Fig. 5a). EC-Earth3 and CanESM5 show a double peak distribution for SIE at the end of SRILEs, consistent with early and late RILEs due to high sea ice variability for EC-Earth3 and the early increase in variability (2010–2015) for CanESM5 (Fig. S5). In contrast, the probability density functions of SIE at RILEs end for March RILEs (MRILEs hereafter) are flatter and wider than the ones for SRILEs (Figs. 4d and 5d), which is explained by the large contribution of model uncertainty on the initial SIE as well as on the duration and intra-seasonal consistency of MRILEs.

In contrast to September, MRILE occurrences are mostly simulated after 2050. The peak of MRILE occurrence is around 2075 and for SIE values around 11 million km^2 in the CMIP6 multi-model ensemble following the high warming scenario (Fig. 4a,b). Among the large ensembles simulating MRILEs (i.e., EC-Earth3, CanESM5, and ACCESS-ESM1-5), the mean SIE at the onset of MRILEs is similar to the CMIP6 multi-model ensemble, except for ACCESS-ESM1-5 for which the peak in MRILE occurrences falls around 15 million km^2 (Fig. 5b). Uncertainty in the timing of MRILEs is more pronounced across these large ensembles (Fig. 5a), highlighting once more the large contribution of model uncertainty on winter RILEs. This uncertainty can be explained by differences in sea ice mean state and/or variability. For example, although the onset years for winter RILEs differ between CanESM5 and EC-Earth3 (Fig. 5a), both large ensembles show an increase in sea ice variability as the March SIE falls below 10 million km^2 (Fig.S5b). In contrast, MPI-ESM1-2-LR exhibits much lower March sea ice variability both as a function of time and SIE (Fig.S5), resulting in few winter RILEs (Fig. 5e). Both ACCESS-ESM1-5 and MIROC6 show an increase in sea ice variability over the last few decades of the 21$^{\mathrm{st}}$ century as they reach lower SIE (Fig.S5), resulting in an increase in the occurrence of winter RILEs at that time (Fig. 3). However, it is important to note that reaching a critical sea ice state is not a sufficient condition for winter RILEs to occur. MIROC6 simulates no winter RILE before the last two decades of the 21$^{\mathrm{st}}$ century (Fig. 3d) despite showing a less extensive and thinner winter ice cover (Figs. 1b and S4b) Holland et al. (2008) showed that, in addition to an adequately thin ice cover, a forcing perturbation is necessary to initiate RILEs in September, and our results suggest that this finding is also applicable to winter RILEs, except for EC-Earth3. Indeed, EC-Earth3 simulates winter RILEs at the end of the 20$^{\mathrm{th}}$ century (Fig. 3e) without meeting the thin sea ice condition.

According to the CMIP6 multi-model ensemble, around 50% of the SRILEs end under 2 million km^2 and 30% between 0 and 1 million km^2 (i.e., consistently ice-free conditions) for both warming scenarios (Fig. 4d). This is also the case for the large ensembles: 18–37% of the SRILES end below the 1 million km^2 threshold (Fig. 5d). For MIROC6, the majority of SRILEs begin at around 2.5 million km^2, which is the lowest value compared to other large ensembles (Fig. 5b). Accordingly, 37% of MIROC6 SRILEs end below 1 million km^2 (Fig. 5d).

A peak of RILE occurrences between 5000 and 7500 km^3 of SIV is evident for both September and March (Fig. 4c) in the CMIP6 multi-model ensemble. Indeed, we find that more than 20% of SRILEs initiate at a SIV ranging from 4000 to 6000

https://doi.org/10.5194/egusphere-2024-1873
Preprint. Discussion started: 1 July 2024

km^3. This is noteworthy considering that the September SIV in 2023 according to the PIOMAS reanalysis dataset was 5000 km^3 (Schweiger et al., 2011). This parity in probability peaks of initial SIV between September and March suggests that the average ice volume state may serve as a preconditionning for RILE occurrences. The explanation for the slight shift of the probability peak for initial SIV toward smaller values for March compared to September likely lies with the fact that most MRILEs happen after the Arctic has reached consistently ice-free conditions in September.

4 Discussion

The increase in RILE occurrence follows the increase in SIE variability, echoing previous findings regarding the influence of large interannual SIE fluctuations on abrupt Arctic SIE declines (Holland et al., 2008; Goosse et al., 2009). This variability is highest when approaching consistently ice-free conditions (Swart et al., 2015; Mioduszewski et al., 2019) with increased SIE variability in summer and autumn attributed to the higher efficiency of open water formation, while variability in November-January is influenced by ice growth (Mioduszewski et al., 2019).

Increased variability in SIE had been found to be linked to declining ice thickness (Holland et al., 2008), particularly in winter, with a complex interplay between climate, ice thickness, and geographical factors (Goosse et al., 2009; Mioduszewski et al., 2019). Our results also suggest a preconditioning role of SIV on RILEs. According to Döscher and Koenigk (2013), RILEs are controlled by the initial SIV at the onset of the melting period and by the onset of specific atmospheric circulation patterns during summer months. In summer months, thinning ice cover in climate models increases ice extent variability, making it more vulnerable to natural variations and amplifying changes due to the surface albedo feedback resulting in an increased probability of extreme events such as RILEs (Döscher and Koenigk, 2013).

Based on the analyzed CMIP6 model simulations, our study suggests that the most probable occurrence of a SRILE would be in mid-2020s, or once we reach a September SIE and SIV mean state of approximately 3.5 million km^2 and 6000 km^3, respectively. By comparison, the observed September mean SIE over the past five years (2019–2023) was approximately 4.5 million km^2 (Fetterer et al., 2017), while the September mean SIV over the past five years was approximately 4600 km^3 (Schweiger et al., 2011). As such, the current sea ice state (SIE and SIV) is close to the projected characteristics of SRILEs in CMIP6 simulations. Additionally, our results based on CMIP6 models suggest that the period of relatively stable Arctic sea ice conditions during 2010–2019 increases the likelihood of observing a SRILE in the real world (Fig. 6). This convergence emphasizes the increasing urgency to comprehend the variability, causes, and impacts of such events. It is important to note, however, that the exact timing and mean state associated with the occurrence of a RILE in the future is still uncertain due to the large contribution of internal climate variability. A deeper examination of the physical mechanisms driving decadal SIE variability in model simulations, through the study of RILEs in the future, is therefore crucial to enhance our capacity to comprehend and predict the evolution of Arctic sea ice in the coming years and decades.

https://doi.org/10.5194/egusphere-2024-1873
Preprint. Discussion started: 1 July 2024

5 Conclusions

Rapid ice loss events (RILEs) were first identified by Holland et al. (2006) and, even though several follow-up studies have been conducted (Lawrence et al., 2008; Holland et al., 2008; Döscher and Koenigk, 2013; Paquin et al., 2013; Auclair and Tremblay, 2018; Mioduszewski et al., 2019; Rieke et al., 2023), we still currently lack a comprehensive overview of the properties of RILEs. Previous studies used a limited number of climate models or mainly focused on one season. Our study assessed RILEs in the Arctic in the past and future during all months of the year using a large set of realizations from five large ensembles and simulations from 26 models participating in CMIP6. The findings illustrate the complex variability of the Arctic sea ice cover through the study of RILEs, shifting from a relatively stable condition in the 20th century to a more unpredictable state as we progress further into the 21st century, especially during summer. Below, we provide a summary of key results:

- Under high emission scenario (SSP5-8.5), RILEs occur in the CMIP6 multi-model ensemble (26 models) and five large ensembles for all months of the year (Figs. 2 and 3). All five large ensembles have at least one ensemble member exhibiting a RILE in every month of the year, except for MIROC6 in April. For the CMIP6 multi-model ensemble, the percentage range of members with at least one RILE across the year goes from 62% to 96% and, with every model experiencing at least one RILE during the analysis period.

- The large number of RILEs simulated by the CMIP6 multi-model ensemble in August, September, and October is similar across both future scenarios but that is not the case over the rest of the year (Nov–Jul), with significantly fewer RILEs when using the SSP1-2.6 scenario (Fig. 4e). This suggests that the choice of forcing has little influence on the probability of occurrence of end-of-summer RILEs but that it plays a dominant role in all other months of the year.

- RILEs in winter last longer toward the end of the century under SSP5-8.5, while they are almost non-existent toward the end of the century in climate projections using SSP1-2.6 (Fig. 2). During the last 6 months of the year, RILEs are more randomly spread than during the first 6 months of the year, indicating a regime difference between different parts of the year. Additionally, it seems that there is a larger influence of model uncertainty for the timing of RILEs in winter.

- The increase in RILE occurrence is driven by the increase in SIE variability (Fig. S5), as already highlighted by Holland et al. (2008) in their analysis of rapid September ice retreat. Our results suggest that this finding is also applicable to winter RILEs. On top of that, the greater the sea ice extent variability is in a model, the more the model simulates RILEs. This result is nicely illustrated by EC-Earth3 (large ensemble), in which there is a high probability (90%) of experiencing more than one RILE (2–5) during the period from 1970 to consistently ice-free conditions.

- SIV values at the onset of RILEs are similar for both March and September RILEs and both scenarios in the CMIP6 multi-model analysis (Fig. 4c). This suggests a preconditioning role of SIV for RILEs with a threshold ranging from 5000 to 7500 km^3.

https://doi.org/10.5194/egusphere-2024-1873
Preprint. Discussion started: 1 July 2024

– There is 20% increase in the probability that a RILE will occur after a 10-year long steady SIE phase (Fig. 6). This increases the probability of a RILE in the near future, following the positive SIE trend period between 2012 and 2023 (0.00168 million km^2 / year)

To conclude, we have shown that RILEs occur in a range from 62% for the months from February to June to 96% for the months from August to November of CMIP6 simulations of the multi-model ensemble. RILEs could occur through all months of the years (and not be restricted to summer only), depending on the future emission scenarios.

Data availability. The data from all CMIP6 models are openly available and can be found on the Earth System Grid Federation (ESGF) nodes: https://esgf-node.llnl.gov/search/CMIP6/. The DOI (Digital Object Identifier) for each model simulation can be found in the Supplementary Materials (Table S1). The PIOMAS (Schweiger et al., 2011) sea-ice volume data can be accessed via the Polar Science Center of the University of Washington: http://psc.apl.uw.edu/research/projects/arctic-sea-ice-volume-anomaly. The observational SIE data from the National Snow and Ice Data Center (NSIDC) can be accessed via https://nsidc.org/data/nsidc-0192/versions/3.

Author contributions. AS, FM, TF and AJ conceptualized the science plan. AS performed the analyses, produced the figures and wrote the manuscript based on the insights from the co-authors. Initial analysis on the seasonality of RILEs and the SIE threshold where RILEs begin to occur were performed in a subset of large ensemble by ES & MO and DQ, respectively, under guidance from CWP and AJ.

Competing interests. The contact author has declared that neither they nor their co-authors have any competing interests.

Acknowledgements. Annelies Sticker and Patricia DeRepentigny are funded by the European Union (ERC, ArcticWATCH, 101040858). Views and opinions expressed are however those of the author(s) only and do not necessarily reflect those of the European Union or the European Research Council Executive Agency. Neither the European Union nor the granting authority can be held responsible for them. François Massonnet is a F.R.S.-FNRS Research Associate. David Docquier is funded by BELSPO through the RESIST project (contract no. RT/23/RESIST). Computational resources have been provided by the supercomputing facilities of the Université catholique de Louvain (CISM/UCL) and the Consortium des Équipements de Calcul Intensif en Fédération Wallonie Bruxelles (CÉCI) funded by the Fond de la Recherche Scientifique de Belgique (F.R.S.–FNRS) under convention 2.5020.11. The contributions of A. Jahn, C. Wyburn-Powell, D. Quint, E. Shivers, and M. Ortiz were supported by NSF-CAREER award 1847398. We acknowledge the World Climate Research Programme's Working Group on Coupled Modelling, which is responsible for CMIP, and we thank the climate modeling groups for producing and making available their model output. We acknowledge the use of ChatGPT (https://chat.openai.com/) to improve the writing style of a few paragraphs.

https://doi.org/10.5194/egusphere-2024-1873
Preprint. Discussion started: 1 July 2024

References

Arrigo, K. and van Dijken, G.: Secular trends in Arctic Ocean net primary production, Journal of Geophysical Research (Oceans), 116, https://doi.org/10.1029/2011JC007151, 2011.

Auclair, G. and Tremblay, L. B.: The Role of Ocean Heat Transport in Rapid Sea Ice Declines in the Community Earth System Model Large Ensemble, Journal of Geophysical Research: Oceans, 123, 8941–8957, https://doi.org/10.1029/2018JC014525, _eprint: https://onlinelibrary.wiley.com/doi/pdf/10.1029/2018JC014525, 2018.

Baxter, I., Ding, Q., Schweiger, A., L'Heureux, M., Baxter, S., Wang, T., Zhang, Q., Harnos, K., Markle, B., Topal, D., and Lu, J.: How Tropical Pacific Surface Cooling Contributed to Accelerated Sea Ice Melt from 2007 to 2012 as Ice Is Thinned by Anthropogenic Forcing, Journal of Climate, 32, 8583 – 8602, https://doi.org/10.1175/JCLI-D-18-0783.1, 2019.

Cavalieri, D. J., Parkinson, C. L., Gloersen, P., and Zwally, H. J.: Sea Ice Concentrations from Nimbus-7 SMMR and DMSP SSM/I-SSMIS Passive Microwave Data, Version 1, https://doi.org/10.5067/8GQ8LZQVL0VL, 1996.

Crawford, A., Stroeve, J., Smith, A., and Jahn, A.: Arctic open-water periods are projected to lengthen dramatically by 2100, Communications Earth and Environment, 2, 109, https://doi.org/10.1038/s43247-021-00183-x, 2021.

Delhaye, S., Msadek, R., Fichefet, T., Massonnet, F., and Terray, L.: Consistent but more intense atmospheric circulation response to Arctic sea ice loss in CMIP6 experiments compared to PAMIP experiments, EGUsphere, 2023, 1–32, https://doi.org/10.5194/egusphere-2023-1748, 2023.

Deser, C., Lehner, F., Rodgers, K., Ault, T., Delworth, T., DiNezio, P., Fiore, A., Frankignoul, C., Fyfe, J., Horton, D., Kay, J., Knutti, R., Lovenduski, N., Marotzke, J., McKinnon, K., Minobe, S., Randerson, J., Screen, J., Simpson, I., and Ting, M.: Insights from Earth system model initial-condition large ensembles and future prospects, Nature Climate Change, 10, 277–286, https://doi.org/10.1038/s41558-020-0731-2, 2020.

Döscher, R. and Koenigk, T.: Arctic rapid sea ice loss events in regional coupled climate scenario experiments, Ocean Science, 9, 217–248, https://doi.org/10.5194/os-9-217-2013, publisher: Copernicus GmbH, 2013.

Fetterer, F., Knowles, K., Meier, W., Savoie, M., and Windnagel, A.: Sea Ice Index, Version 3 [monthly values from 1979 to 2023], https://doi.org/10.7265/N5K072F8, accessed Apr 2024, 2017.

Francis, J. A. and Wu, B.: Why has no new record-minimum Arctic sea-ice extent occurred since September 2012?, Environmental Research Letters, 15, 114 034, https://doi.org/10.1088/1748-9326/abc047, 2020.

Goosse, H., Arzel, O., Bitz, C. M., de Montety, A., and Vancoppenolle, M.: Increased variability of the Arctic summer ice extent in a warmer climate, Geophysical Research Letters, 36, https://doi.org/https://doi.org/10.1029/2009GL040546, 2009.

Holland, M. M., Bitz, C. M., and Tremblay, B.: Future abrupt reductions in the summer Arctic sea ice, Geophysical Research Letters, 33, https://doi.org/10.1029/2006GL028024, _eprint: https://onlinelibrary.wiley.com/doi/pdf/10.1029/2006GL028024, 2006.

Holland, M. M., Bitz, C. M., Tremblay, L.-B., and Bailey, D. A.: The Role of Natural Versus Forced Change in Future Rapid Summer Arctic Ice Loss, pp. 133–150, American Geophysical Union (AGU), ISBN 9781118666470, https://doi.org/https://doi.org/10.1029/180GM10, 2008.

Jahn, A., Holland, M. M., and Kay, J. E.: Projections of an ice-free Arctic Ocean, Nat. Rev. Earth Environ., 5, 164–176, 2024.

Kay, J., Holland, M., and Jahn, A.: Inter-annual to multi-decadal Arctic sea ice extent trends in a warming world, Geophysical Research Letters, 38, L15 708, https://doi.org/10.1029/2011GL048008, 2011.

https://doi.org/10.5194/egusphere-2024-1873
Preprint. Discussion started: 1 July 2024

Landrum, L. and Holland, M.: Extremes become routine in an emerging new Arctic, Nature Climate Change, 10, 1–8, https://doi.org/10.1038/s41558-020-0892-z, 2020.

Lawrence, D. M., Slater, A. G., Tomas, R. A., Holland, M. M., and Deser, C.: Accelerated Arctic land warming and permafrost degradation during rapid sea ice loss, Geophysical Research Letters, 35, https://doi.org/10.1029/2008GL033985, _eprint: https://onlinelibrary.wiley.com/doi/pdf/10.1029/2008GL033985, 2008.

Lin, X., Massonnet, F., Fichefet, T., and Vancoppenolle, M.: SITool (v1.0) – a new evaluation tool for large-scale sea ice simulations: application to CMIP6 OMIP, Geoscientific Model Development, 14, 6331–6354, https://doi.org/10.5194/gmd-14-6331-2021, 2021.

Meredith, M., Sommerkorn, M., Cassotta, S., Derksen, C., Ekaykin, A., Hollowed, A., Kofinas, G., Mackintosh, A., Melbourne-Thomas, J., Muelbert, M., Ottersen, G., Pritchard, H., and Schuur, E.: Polar Regions, in: IPCC Special Report on the Ocean and Cryosphere in a Changing Climate, edited by Pörtner, H.-O., Roberts, D., Masson-Delmotte, V., Zhai, P., Tignor, M., Poloczanska, E., Mintenbeck, K., Alegrí´a, A., Nicolai, M., Okem, A., Petzold, J., Rama, B., and NM, W., pp. 203–320, Cambridge University Press, Cambridge, UK and New York, NY, USA, 2019.

Mioduszewski, J. R., Vavrus, S., Wang, M., Holland, M., and Landrum, L.: Past and future interannual variability in Arctic sea ice in coupled climate models, The Cryosphere, 13, 113–124, https://doi.org/10.5194/tc-13-113-2019, publisher: Copernicus GmbH, 2019.

Notz, D.: Sea-ice extent and its trend provide limited metrics of model performance, The Cryosphere, 8, 229–243, https://doi.org/10.5194/tc-8-229-2014, publisher: Copernicus GmbH, 2014.

Olonscheck, D., Suarez-Gutierrez, L., Milinski, S., Beobide-Arsuaga, G., Baehr, J., Fröb, F., Ilyina, T., Kadow, C., Krieger, D., Li, H., Marotzke, J., Plésiat, E., Schupfner, M., Wachsmann, F., Wallberg, L., Wieners, K.-H., and Brune, S.: The New Max Planck Institute Grand Ensemble With CMIP6 Forcing and High-Frequency Model Output, Journal of Advances in Modeling Earth Systems, 15, e2023MS003 790, https://doi.org/https://doi.org/10.1029/2023MS003790, e2023MS003790 2023MS003790, 2023.

Onarheim, I. H., Eldevik, T., Smedsrud, L. H., and Stroeve, J. C.: Seasonal and Regional Manifestation of Arctic Sea Ice Loss, Journal of Climate, 31, 4917 – 4932, https://doi.org/10.1175/JCLI-D-17-0427.1, 2018.

O'Neill, B. C., Tebaldi, C., van Vuuren, D. P., Eyring, V., Friedlingstein, P., Hurtt, G., Knutti, R., Kriegler, E., Lamarque, J.-F., Lowe, J., Meehl, G. A., Moss, R., Riahi, K., and Sanderson, B. M.: The Scenario Model Intercomparison Project (ScenarioMIP) for CMIP6, Geoscientific Model Development, 9, 3461–3482, https://doi.org/10.5194/gmd-9-3461-2016, 2016.

Paquin, J.-P., Döscher, R., Koenigk, T., and Sushama, L.: Causes and consequences of mid-21st-century rapid ice loss events simulated by the Rossby centre regional atmosphere-ocean model, Tellus, 65, https://doi.org/10.3402/tellusa.v65i0.19110, 2013.

Polyakov, I., Ingvaldsen, R., Pnyushkov, A., Bhatt, U., Francis, J., Janout, M., Kwok, R., and Skagseth, Ø.: Fluctuating Atlantic inflows modulate Arctic atlantification, Science (New York, N.Y.), 381, 972–979, https://doi.org/10.1126/science.adh5158, 2023.

Rieke, O., Årthun, M., and Dörr, J. S.: Rapid sea ice changes in the future Barents Sea, The Cryosphere, 17, 1445–1456, https://doi.org/10.5194/tc-17-1445-2023, 2023.

Schweiger, A., Lindsay, R., Zhang, J., Steele, M., Stern, H., and Kwok, R.: Uncertainty in modeled Arctic sea ice volume, JOURNAL OF GEOPHYSICAL RESEARCH-OCEANS, 116, https://doi.org/10.1029/2011JC007084, 2011.

Screen, J., Deser, C., and Sun, L.: Projected changes in regional climate extremes arising from Arctic sea ice loss, Environmental Research Letters, 10, https://doi.org/10.1088/1748-9326/10/8/084006, 2015.

Serreze, M. C. and Barry, R. G.: Processes and impacts of Arctic amplification: A research synthesis, Global and Planetary Change, 77, 85–96, https://doi.org/https://doi.org/10.1016/j.gloplacha.2011.03.004, 2011.

https://doi.org/10.5194/egusphere-2024-1873
Preprint. Discussion started: 1 July 2024

Serreze, M. C., Barrett, A. P., Stroeve, J. C., Kindig, D. N., and Holland, M. M.: The emergence of surface-based Arctic amplification, The Cryosphere, 3, 11–19, https://doi.org/10.5194/tc-3-11-2009, 2009.

Shen, Z., Duan, A., Li, D., and Li, J.: Assessment and Ranking of Climate Models in Arctic Sea Ice Cover Simulation: From CMIP5 to CMIP6, Journal of Climate, 34, 3609 – 3627, https://doi.org/10.1175/JCLI-D-20-0294.1, 2021.

Shiogama, H., Tatebe, H., Hayashi, M., Abe, M., Arai, M., Koyama, H., Imada, Y., Kosaka, Y., Ogura, T., and Watanabe, M.: MIROC6 Large Ensemble (MIROC6-LE): experimental design and initial analyses, Earth System Dynamics, 14, 1107–1124, https://doi.org/10.5194/esd-14-1107-2023, 2023.

Shu, Q., Wang, Q., Song, Z., Qiao, F., Zhao, J., Chu, M., and Li, X.: Assessment of Sea Ice Extent in CMIP6 With Comparison to Observations and CMIP5, Geophysical Research Letters, 47, e2020GL087 965, https://doi.org/https://doi.org/10.1029/2020GL087965, e2020GL087965 2020GL087965, 2020.

SIMIP Community: Arctic Sea Ice in CMIP6, Geophysical Research Letters, 47, https://doi.org/10.1029/2019GL086749, 2020.

Stroeve, J. and Notz, D.: Insights on past and future sea-ice evolution from combining observations and models, Global and Planetary Change, 135, https://doi.org/10.1016/j.gloplacha.2015.10.011, 2015.

Stroeve, J. and Notz, D.: Changing state of Arctic sea ice across all seasons, Environmental Research Letters, 13, 103 001, https://doi.org/10.1088/1748-9326/aade56, 2018.

Swart, N. C., Fyfe, J. C., Hawkins, E., Kay, J. E., and Jahn, A.: Influence of internal variability on Arctic sea-ice trends, Nature Climate Change, 5, 86–89, https://doi.org/10.1038/nclimate2483, number: 2 Publisher: Nature Publishing Group, 2015.

Swart, N. C., Cole, J. N. S., Kharin, V. V., Lazare, M., Scinocca, J. F., Gillett, N. P., Anstey, J., Arora, V., Christian, J. R., Hanna, S., Jiao, Y., Lee, W. G., Majaess, F., Saenko, O. A., Seiler, C., Seinen, C., Shao, A., Sigmond, M., Solheim, L., von Salzen, K., Yang, D., and Winter, B.: The Canadian Earth System Model version 5 (CanESM5.0.3), Geoscientific Model Development, 12, 4823–4873, https://doi.org/10.5194/gmd-12-4823-2019, 2019.

Taylor, P. C., Cai, M., Hu, A., Meehl, J., Washington, W., and Zhang, G. J.: A Decomposition of Feedback Contributions to Polar Warming Amplification, Journal of Climate, 26, 7023 – 7043, https://doi.org/10.1175/JCLI-D-12-00696.1, 2013.

Wassmann, P., Duarte, C. M., Agusti, S., and Sejr, M. K.: Footprints of climate change in the Arctic marine ecosystem, Global Change Biology, 17, 1235–1249, https://doi.org/https://doi.org/10.1111/j.1365-2486.2010.02311.x, 2011.

Watts, M., Maslowski, W., Lee, Y. J., Kinney, J. C., and Osinski, R.: A Spatial Evaluation of Arctic Sea Ice and Regional Limitations in CMIP6 Historical Simulations, Journal of Climate, 34, 6399–6420, https://doi.org/10.1175/JCLI-D-20-0491.1, aDS Bibcode: 2021JCli...34.6399W, 2021.

Wyser, K., Koenigk, T., Fladrich, U., Fuentes-Franco, R., Karami, M. P., and Kruschke, T.: The SMHI Large Ensemble (SMHI-LENS) with EC-Earth3.3.1, Geoscientific Model Development, 14, 4781–4796, https://doi.org/10.5194/gmd-14-4781-2021, 2021.

Ziehn, T., Chamberlain, M., Law, R., Lenton, A., Bodman, R., Dix, M., Stevens, L., Wang, Y., and Srbinovsky, J.: The Australian Earth System Model: ACCESS-ESM1.5, Journal of Southern Hemisphere Earth Systems Science, 70, https://doi.org/10.1071/ES19035, 2020.

https://doi.org/10.5194/egusphere-2024-1873
Preprint. Discussion started: 1 July 2024

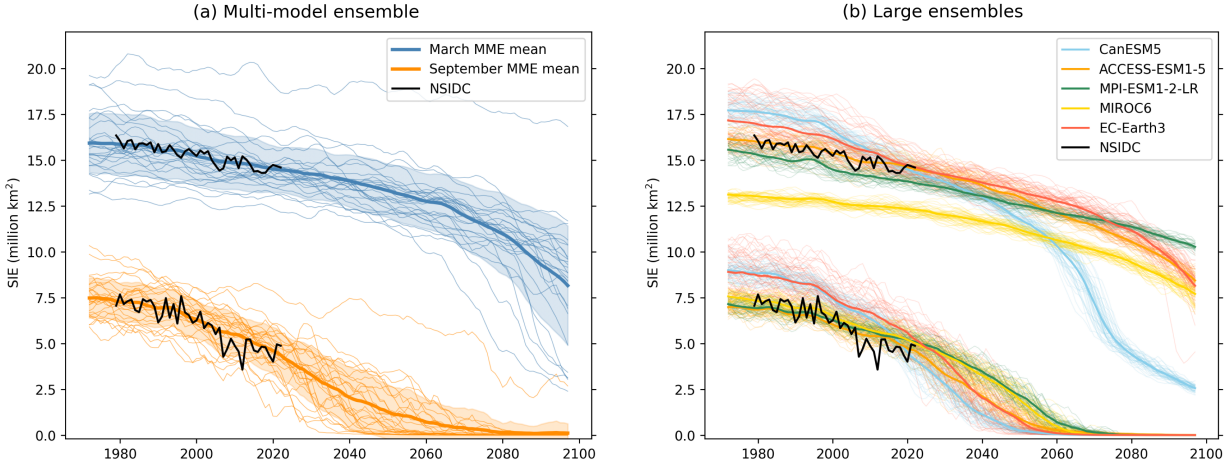

Figure 1. March (top lines) and September (bottom lines) 5-year running mean SIE evolution over the historical period and high emission scenario SSP5-8.5 for (a) the CMIP6 multi-model ensemble (26 models, 1 member per model), with thin lines representing individual models, thick lines the multi-model ensemble mean, and shaded areas one standard deviation across the multi-model ensemble, and (b) 5 large ensembles with thin lines representing individual ensemble members and thick lines the ensemble mean. The black lines show the observations from NISDC.

https://doi.org/10.5194/egusphere-2024-1873
Preprint. Discussion started: 1 July 2024

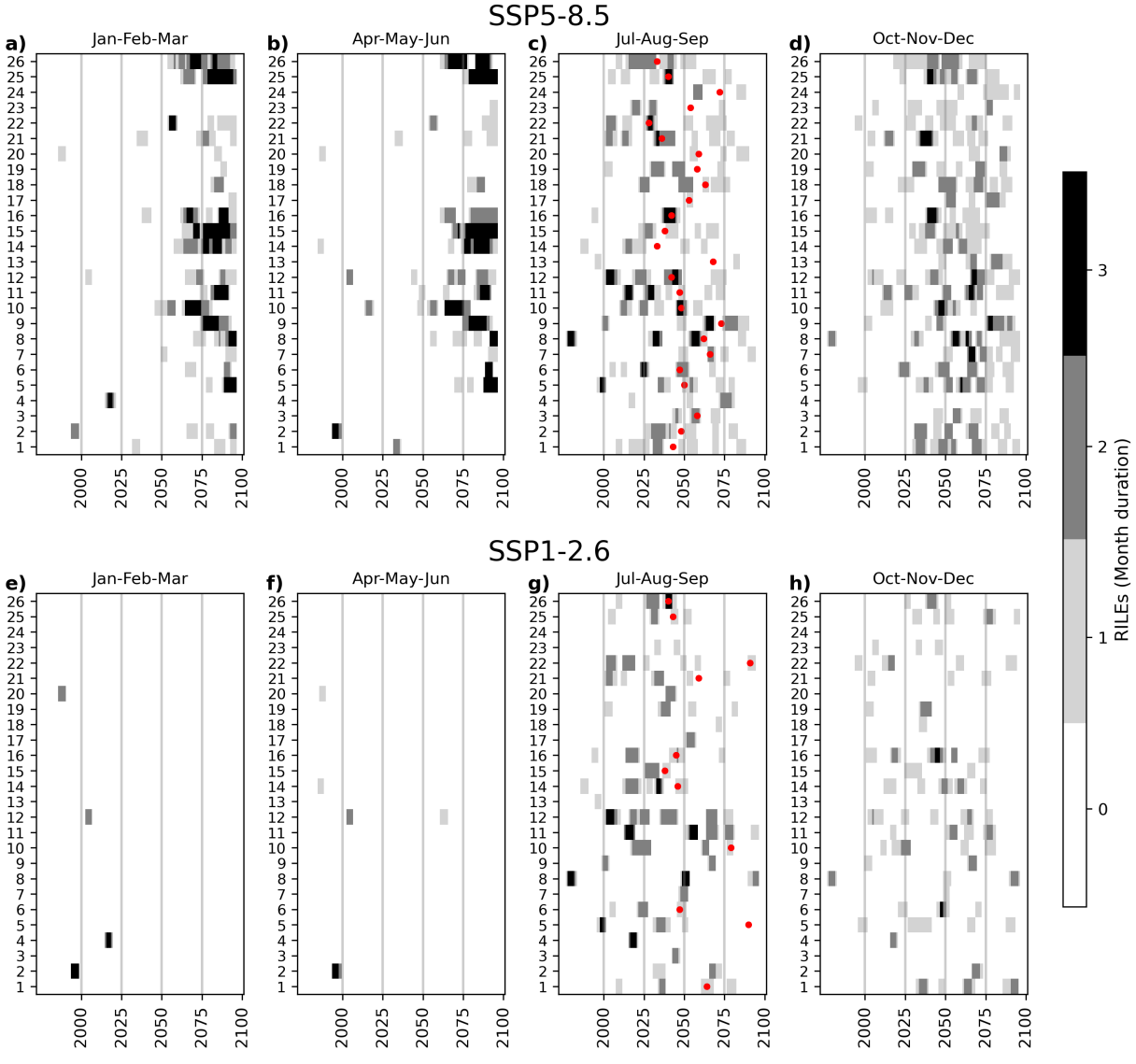

Figure 2. Occurrences of RILEs from 1970–2099 in the first ensemble member of the 26 different CMIP6 models following the SSP5-8.5 (top row) and SSP1-2.6 (bottom row) scenarios. Each panel shows a period of three months, with light grey representing RILEs occurring over one of the three months, dark grey representing RILEs occurring over two of the three months, and black representing RILEs occurring over all three months of the season. The numbers on the y-axis refer to the 26 different models listed in Table 1. Red dots in the Jul-Aug-Sep panels indicate the first year of consistently ice-free conditions in September (i.e., first year of five consecutive years when the smoothed September SIE falls below 1 million km^2).

https://doi.org/10.5194/egusphere-2024-1873
Preprint. Discussion started: 1 July 2024

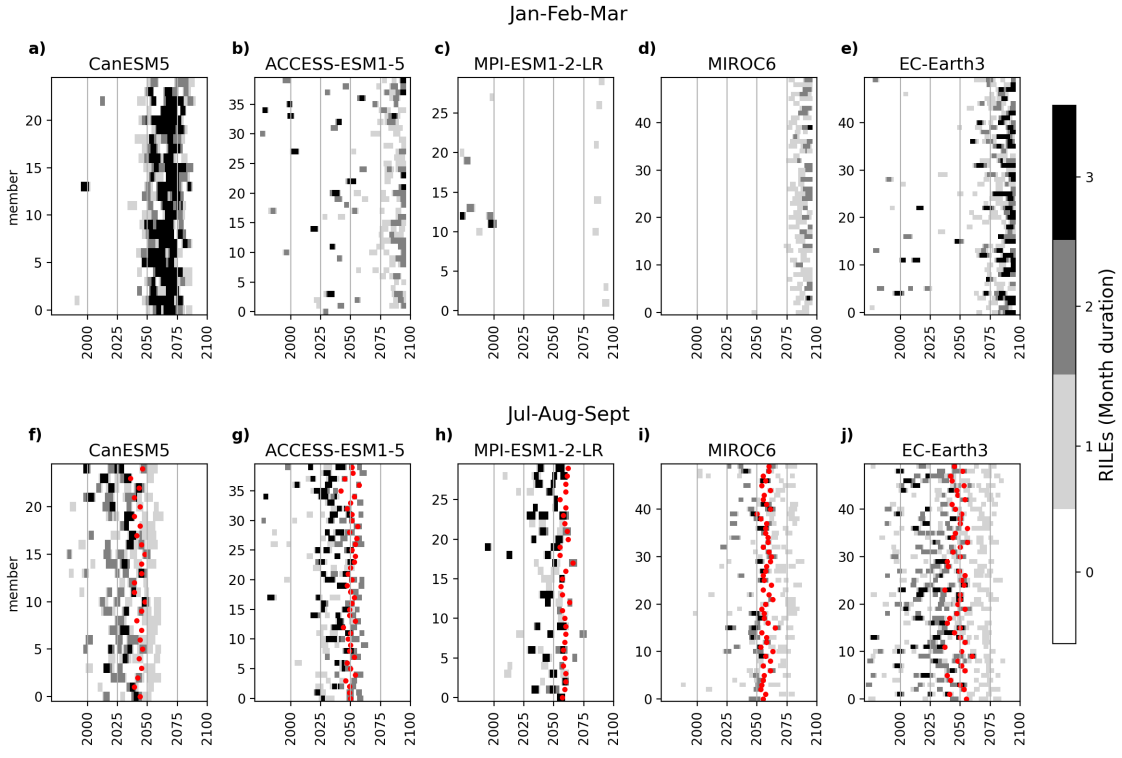

Figure 3. Same as in Fig. 2 but for the periods Jan-Feb-Mar (top row) and Jul-Aug-Sep (bottom row) in the five large ensembles following the SSP5-8.5 scenario.

https://doi.org/10.5194/egusphere-2024-1873
Preprint. Discussion started: 1 July 2024

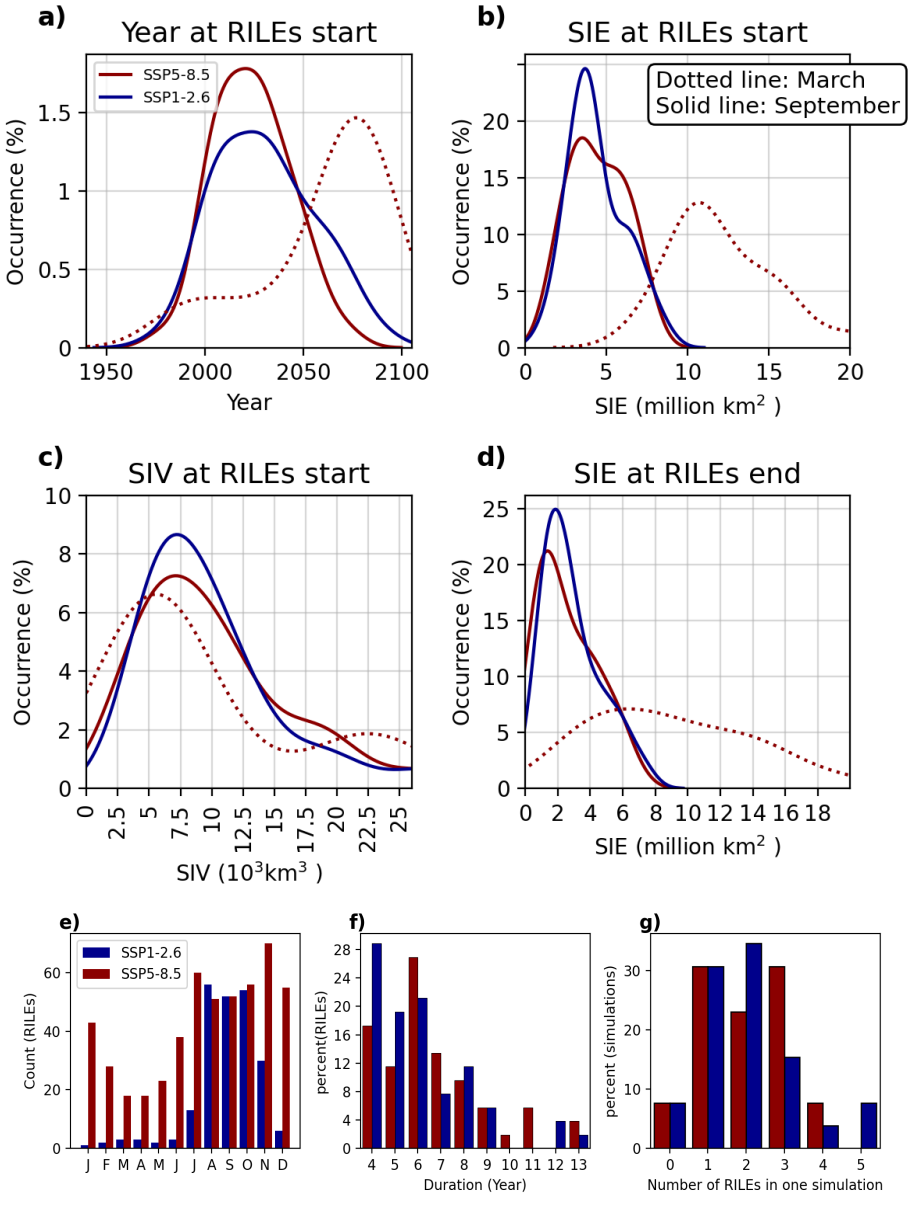

Figure 4. RILEs characteristics in the CMIP6 multi-model ensemble: probability density function of the (a) years, (b) SIE and (c) SIV at which RILEs begin, and (d) the SIE at which RILEs end for September (solid lines) and March (dotted lines), (e) total number of RILEs per month, (f) percentage of SRILEs as a function of their duration in years, and (g) percentage of SRILEs per simulation for the CMIP6 multi-model ensemble over 1970–2099 under the high (red) and low (blue) warming scenarios. Note that we do not show results for the low warming scenario in March in panels (a)-(d) due to very few RILEs being simulated.

https://doi.org/10.5194/egusphere-2024-1873
Preprint. Discussion started: 1 July 2024

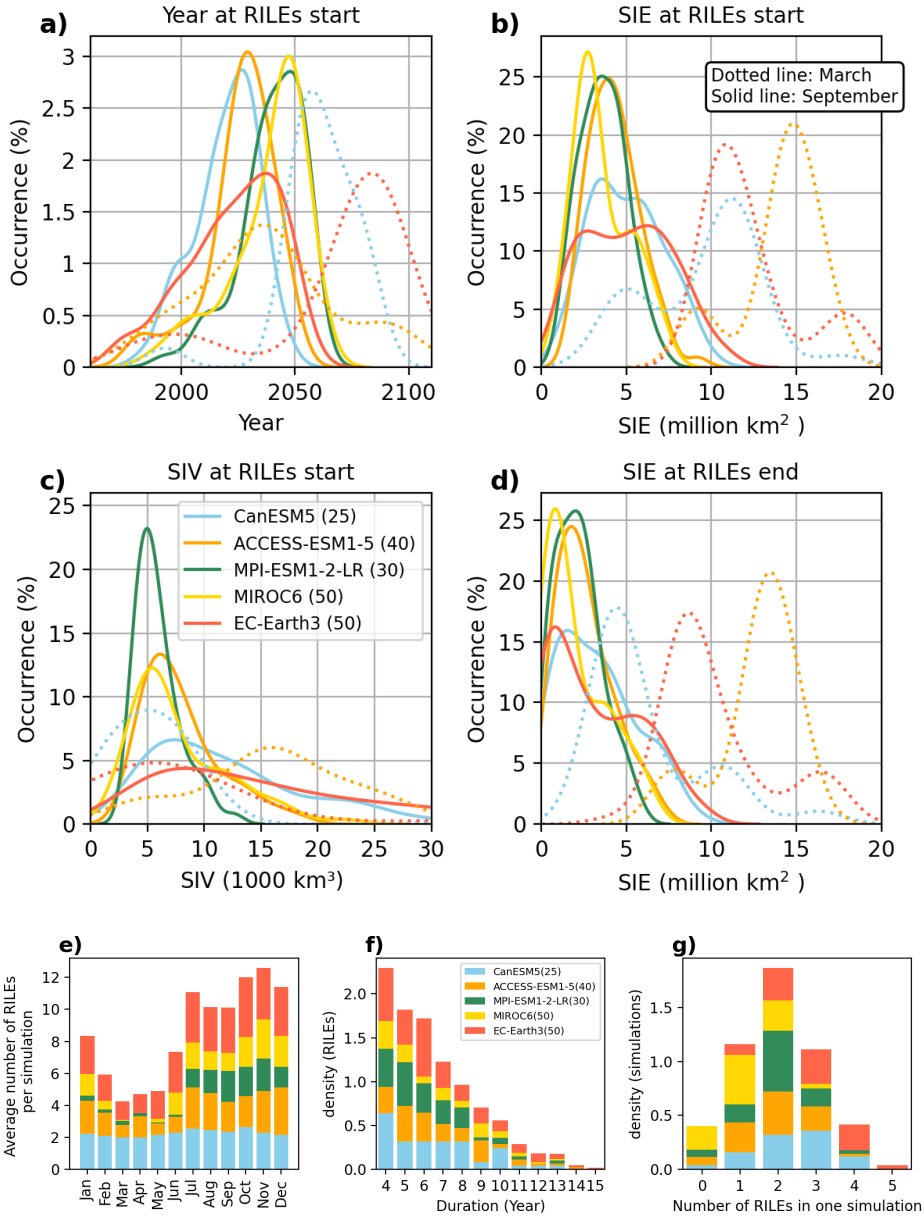

Figure 5. Same as Fig. 4 but for the five large ensembles following the high emission scenario SSP5-8.5. The numbers in parentheses in the legend indicates the ensemble size for each large ensemble. Note that we do not show results for MPI-ESM1-2-LR and MIROC6 in March in panels (a)-(d) due to very few MRILEs being simulated in these two models.

https://doi.org/10.5194/egusphere-2024-1873
Preprint. Discussion started: 1 July 2024

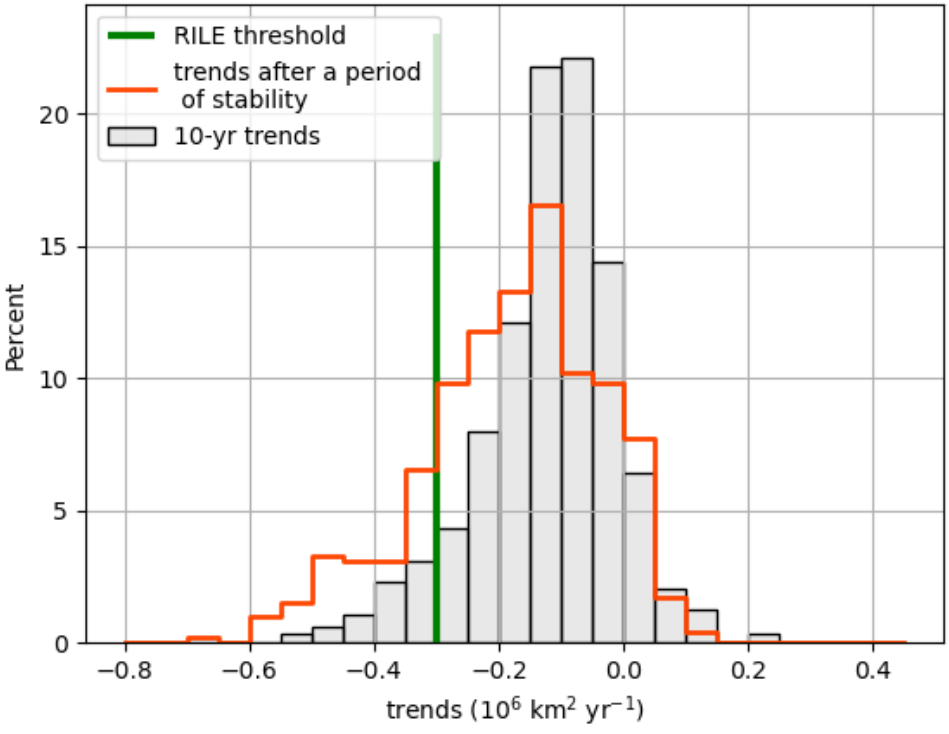

Figure 6. Distribution of all possible 10-year Arctic September SIE trends (grey) and trends after a period of stability (orange) for the CMIP6 multi-model ensemble from 2015 to consistently ice-free conditions using SSP5-8.5 scenario. A period of stability is defined as a 10-year period with a neutral or positive SIE trend. The 10-year trends are computed on the 5-year running mean SIE timeseries. The solid green line indicates the threshold used to define a RILE (see section 2.3 for more details). Fig. S6 shows similar results but for the five large ensembles.

https://doi.org/10.5194/egusphere-2024-1873
Preprint. Discussion started: 1 July 2024

Table 1. Ocean and sea ice components, together with their nominal resolution, of the CMIP6 models used in this analysis. The resolution corresponds to the ocean/sea ice component. The sea ice component for models #19–20 is unnamed but uses the "Semtner zero-layer" thermodynamic and "Hibler 79" dynamic schemes.

MODEL NAME	OCEAN MODEL	SEA ICE MODEL	OCEAN / SEA ICE RESOLUTION
1. ACCESS-CM2	MOM5	CICE5.1.2	100 km
2. ACCESS-ESM1-5	MOM5	CICE 4.1	100 km
3. BCC-CSM2-MR	MOM4	SIS2	50 km
4. CAMS-CSM1-0	MOM4	SIS1.0	100 km
5. CESM2-WACCM	POP 2	CICE 5.1	100 km
6. CESM2	POP 2	CICE 5.1	100 km
7. CNRM-CM6-1-HR	NEMO 3.6	Gelato 6.1	25 km
8. CNRM-CM6-1	NEMO 3.6	Gelato 6.1	100 km
9. CNRM-ESM2-1	NEMO 3.6	Gelato 6.1	100 km
10. CanESM5	NEMO3.4.1	LIM2	100 km
11. EC-Earth3-Veg	NEMO 3.6	NEMO-LIM3	100 km
12. EC-Earth3	NEMO 3.6	NEMO-LIM3	100 km
13. GFDL-ESM4	GFDL-OM4p5	GFDL-SIM4p5	50 km
14. HadGEM3-GC31-LL	NEMO-HadGEM3-GO6.0	CICE-HadGEM3-GSI8	100 km
15. HadGEM3-GC31-MM	NEMO-HadGEM3-GO6.0	CICE-HadGEM3-GSI8	25 km
16. IPSL-CM6A-LR	NEMO 3.6	NEMO-LIM 3	100 km
17. MIROC-ES2L	COCO4.9	COCO4.9	100 km
18. MIROC6	COCO4.9	COCO4.9	100 km
19. MPI-ESM1-2-HR	MPIOMI 1.6.3	Unnamed	50 km
20. MPI-ESM1-2-LR	MPIOMI 1.6.3	Unnamed	250 km
21. MRI-ESM2-0	MRI.COM 4.4	MRI.COM 4.4	100 km
22. NESM3	NEMO v3.4	CICE4.1	100 km
23. NorESM2-LM	MICOM	CICE	100 km
24. NorESM2-MM	MICOM	CICE	100 km
25. TaiESM1	POP2	CICE4	50 km
26. UKESM1-0-LL	NEMO-HadGEM3-GO6.0	CICE-HadGEM3-GS18	100 km